Smart Structures and Systems, Vol. 6, No. 9 (2010) 1057-1077
DOI: http://dx.doi.org/10.12989/sss.2010.6.9.1057

Comparison of various structural damage tracking techniques based on experimental data

Hongwei Huang*[1a], Jann N. Yang[2b] and Li Zhou[3b]

[1]*State Key Laboratory for Disaster Reduction in Civil Engineering, Tongji University, Siping Rd. 1239, Shanghai, China 200092*
[2]*Department of Civil and Environmental Engineering, University of California, Irvine, CA 92697, USA*
[3]*College of Aerospace Engineering, Nanjing University of Aeronautics and Astronautics, Nanjing, China 210016*

(Received July 28, 2009, Accepted June 16, 2010)

Abstract. An early detection of structural damages is critical for the decision making of repair and replacement maintenance in order to guarantee a specified structural reliability. Consequently, the structural damage detection, based on vibration data measured from the structural health monitoring (SHM) system, has received considerable attention recently. The traditional time-domain analysis techniques, such as the least square estimation (LSE) method and the extended Kalman filter (EKF) approach, require that all the external excitations (inputs) be available, which may not be the case for some SHM systems. Recently, these two approaches have been extended to cover the general case where some of the external excitations (inputs) are not measured, referred to as the adaptive LSE with unknown inputs (ALSE-UI) and the adaptive EKF with unknown inputs (AEKF-UI). Also, new analysis methods, referred to as the adaptive sequential non-linear least-square estimation with unknown inputs and unknown outputs (ASNLSE-UI-UO) and the adaptive quadratic sum-squares error with unknown inputs (AQSSE-UI), have been proposed for the damage tracking of structures when some of the acceleration responses are not measured and the external excitations are not available. In this paper, these newly proposed analysis methods will be compared in terms of accuracy, convergence and efficiency, for damage identification of structures based on experimental data obtained through a series of laboratory tests using a scaled 3-story building model with white noise excitations. The capability of the ALSE-UI, AEKF-UI, ASNLSE-UI-UO and AQSSE-UI approaches in tracking the structural damages will be demonstrated and compared.

Keywords: structural health monitoring; structural identification; damage tracking of structures; unknown excitations; experimental verification.

1. Introduction

A rapid assessment of the state (or damage) of the structure is important after a major event, such as a strong earthquake, for post-event emergency responses, rescues and management. In this regard, appropriate data analysis techniques are needed to interpret the vibration data and to identify the state of the structure and its damage on-line or almost on-line. Various time-domain analysis approaches for system identification and damage detection have been proposed in the literature (e.g., Doebling *et al*. 1998, Alvin *et al.* 2003, Bernal and Beck 2004, Chang 2005). Recently, several adaptive

*Corresponding Author, Assistant Professor, E-mail: hongweih@tongji.edu.cn
[a]Assistant Professor
[b]Professor

time-domain damage identification methodologies have been developed (e.g., Huang 2006, Yang and Lin 2005, Yang *et al*. 2006a, b, 2009).

The traditional time-domain analysis techniques, such as the least square estimation (LSE) method (e.g., Goodwin and Sin 1984, Loh *et al*. 2000, Lin *et al*. 2001, Smyth *et al*. 2002, Yang and Lin 2004) and the extended Kalman filter (EKF) approach (e.g., Hoshiya and Saito 1984, Sato *et al*. 2001), require that all the external excitations (inputs) be available from sensor measurements. Due to practical limitations, it may not be possible to install enough sensors in the health monitoring system to measure all the external excitations (inputs), or the external excitations may not be measurable, such as wind or traffic loads. Consequently, it is highly desirable to develop damage identification methodologies utilizing only incomplete measurements, including unmeasured inputs and outputs, in order to reduce the number of sensors required in the health monitoring system.

When the external excitations are not measured or not available, numerical iterative procedures based on the least square estimation (LSE) or the extended Kalman filter (EKF) have been proposed to identify the constant structural parameters (e.g., Wang and Haldar 1994, 1997) without any analytical solutions. Without the measurements of external excitations, adaptive damage tracking methodologies with analytical recursive solutions have been proposed recently to identify the structural damage based on: (i) the LSE approach (Yang *et al.* 2007a), (ii) the extended Kalman filter technique (Yang *et al.* 2007b), (iii) the sequential non-linear least-square estimation (SNLSE) (Yang and Huang 2007), and (iv) the quadratic sum-squares error (QSSE) (Huang 2006, Huang *et al.* 2010). These methodologies are applicable to both linear and nonlinear structures, and are capable of identifying either constant or time-varying structural parameters.

In this paper, the capability of tracking the structural parameters and their variations due to damages for various damage tracking techniques mentioned above are compared based on experimental data. A series of experimental tests using a scaled 3-story building model was conducted in which the white noise excitations were applied to the top floor (Zhou *et al.* 2008). In these experimental tests, an innovative stiffness element device was proposed to simulate structural damages in some stories during the test. Different damage scenarios had been simulated and tested. The experimental data thus obtained (Zhou *et al.* 2008) will be used to verify the capability of the adaptive LSE-UI, EKF-UI, SNLSE-UI-UO and QSSE-UI approaches for the tracking of structural damages. Finally, the identification results for the stiffness of all stories, based on each approach, will be compared with the referenced values predicted by the finite-element analysis. The advantages and drawbacks of each damage tracking approach will be evaluated in terms of the accuracy, efficiency and practicality.

2. Time-domain analysis methodologies without external excitations

The equation of motion of a m-DOF nonlinear structure can be expressed as

$$\mathbf{M}\,\ddot{\mathbf{x}}(t) + \mathbf{F}_c\,[\dot{\mathbf{x}}(t),\boldsymbol{\theta}] + \mathbf{F}_s\,[\mathbf{x}(t),\boldsymbol{\theta}] = \boldsymbol{\eta}^*\mathbf{f}^*(t) + \boldsymbol{\eta}\,\mathbf{f}(t) \tag{1}$$

in which $\mathbf{M}$ = (m×m) mass matrix; $\mathbf{x}(t) = [x_1, x_2,..., x_m]^T$ = m-displacement vector; $\mathbf{F}_c[\dot{\mathbf{x}}(t),\theta]$ = m-damping force vector; $\mathbf{F}_s[\mathbf{x}(t),\theta]$ = m-stiffness force vector; $\mathbf{f}(t)$ = $\bar{m}$ -known (or measured) excitation vector; $\boldsymbol{\eta}$ = m × $\bar{m}$ excitation influence matrix for $\mathbf{f}(t)$; $\mathbf{f}^*(t)$ = r-unknown (or unmeasured) excitation vector; and $\boldsymbol{\eta}^*$ = (m×r) excitation influence matrix for $\mathbf{f}^*(t)$. In Eq. (1), $\theta=[\theta_1, \theta_2,..., \theta_n]^T$ is an n-unknown parametric vector with θ_i (i = 1, 2,..., n) being the ith unknown parameter of the structure, including damping, stiffness, nonlinear and hysteretic parameters. For simplicity of derivation, we shall assume for the time being that the unknown parametric vector $\boldsymbol{\theta}$ is constant, i.e., $\boldsymbol{\theta} = \boldsymbol{\theta}_1 = \boldsymbol{\theta}_2 = ... = \boldsymbol{\theta}_{k+1}$, where $\boldsymbol{\theta}_i = \boldsymbol{\theta}$ ($t = i\Delta t$) for i = 1, 2,..., k+1. In the formulation above, the mass matrix **M** is assumed to be known and constant for simplicity of presentation. The masses can be considered as unknown, in which case the unknown masses will be included in the parametric vector $\boldsymbol{\theta}(t)$ above. Likewise, $\boldsymbol{\eta}^*$ is a null matrix if all excitations are measured, and $\boldsymbol{\eta}$ is a null matrix if all excitations are not measured. In what follows, the bold face letter represents either a vector or a matrix.

2.1 Least square estimation with unknown inputs (LSE-UI)

In this approach, the acceleration, velocity and displacement response vectors, denoted as $\ddot{\mathbf{x}}$, $\dot{\mathbf{x}}$ and $\mathbf{x}$, respectively, are available, and some external excitations are not measured. The observation equation associated with the equation of motion in Eq. (1) can be expressed as

$$\boldsymbol{\varphi}[\dot{\mathbf{x}}(t),\ \mathbf{x}(t);\ t]\boldsymbol{\theta}(t) + \boldsymbol{\varepsilon}(t) = \boldsymbol{\eta}^*\mathbf{f}^*(t) + \mathbf{y}(t) \tag{2}$$

in which $\boldsymbol{\varepsilon}(t)$ is a m-model noise vector, taking into account the model uncertainty of the structure and the measurement noises, $\boldsymbol{\varphi}[\ ]$ is a (m×n) observation matrix composed of the system response vectors, and $\mathbf{y}(t) = \boldsymbol{\eta}\mathbf{f}(t) - \mathbf{M}\ddot{\mathbf{x}}(t)$ is a m-measured vector.

At the time instant $t = (k+1)\Delta t$ with Δt being the sampling interval, Eq. (2) can be written as

$$\boldsymbol{\varphi}_{k+1}\boldsymbol{\theta}_{k+1} + \boldsymbol{\varepsilon}_{k+1} - \boldsymbol{\eta}^*\mathbf{f}^*_{k+1} = \mathbf{y}_{k+1} \tag{3}$$

in which $\boldsymbol{\varphi}_{k+1}$, $\mathbf{y}_{k+1}$, $\boldsymbol{\varepsilon}_{k+1}$ and $\mathbf{f}^*_{k+1}$ are $\boldsymbol{\varphi}[\dot{\mathbf{x}}(t), \mathbf{x}(t); t]$, $\mathbf{y}(t)$, $\boldsymbol{\varepsilon}(t)$ and $\mathbf{f}^*(t)$ at $t = (k+1)\Delta t$, respectively; and $\boldsymbol{\theta}_{k+1} = [\theta_1(k+1), \theta_2(k+1), ..., \theta_n(k+1)]^T$ is the unknown parametric vector with the jth element $\theta_j(k+1) = \theta_j[(k+1)\Delta t]$.

Define an extended unknown vector $\boldsymbol{\theta}_{e,k+1}$ and an extended observation matrix $\boldsymbol{\varphi}_{e,k+1}$ at $t = (k+1)\Delta t$, i.e.,

$$\boldsymbol{\theta}_{e,k+1} = \begin{bmatrix} \boldsymbol{\theta}_{k+1} \\ \hdashline \mathbf{f}^*_{k+1} \end{bmatrix}; \quad \boldsymbol{\varphi}_{e,k+1} = [\boldsymbol{\varphi}_{k+1} \ \vdots \ -\boldsymbol{\eta}^*] \tag{4}$$

in which $\boldsymbol{\theta}_{e,k+1}$ is a (n+r)-unknown vector. Then, Eq. (3) can expressed as

$$\boldsymbol{\varphi}_{e,k+1}\boldsymbol{\theta}_{e,k+1} + \boldsymbol{\varepsilon}_{k+1} = \mathbf{y}_{k+1} \tag{5}$$

Let $\hat{\boldsymbol{\theta}}_{k+1}$ and $\hat{\mathbf{f}}^*_{k+1|k+1}$ be the estimates of $\boldsymbol{\theta}_{k+1}$ and $\mathbf{f}^*_{k+1}$ at $t = t_{k+1} = (k+1)\Delta t$ respectively. The recursive solutions for $\hat{\boldsymbol{\theta}}_{k+1}$ and $\hat{\mathbf{f}}^*_{k+1|k+1}$ can be derived can be derived from as follows (Yang *et al.* 2007a)

$$\hat{\boldsymbol{\theta}}_{k+1} = \hat{\boldsymbol{\theta}}_k + \mathbf{K}_{\boldsymbol{\theta},k+1}\left[\mathbf{y}_{k+1} - \boldsymbol{\varphi}_{k+1}\hat{\boldsymbol{\theta}}_k + \boldsymbol{\eta}^*\hat{\mathbf{f}}^*_{k+1|k+1}\right] \tag{6}$$

$$\hat{\mathbf{f}}^*_{k+1|k+1} = -\mathbf{S}_{k+1}\boldsymbol{\eta}^{*T}[\mathbf{I} - \boldsymbol{\varphi}_{k+1}\mathbf{K}_{\boldsymbol{\theta},k+1}](\mathbf{y}_{k+1} - \boldsymbol{\varphi}_{k+1}\hat{\boldsymbol{\theta}}_k) \tag{7}$$

in which

$$\mathbf{K}_{\boldsymbol{\theta},k+1} = \mathbf{P}_{\boldsymbol{\theta},k}\boldsymbol{\varphi}^T_{k+1}\left[\mathbf{I} + \boldsymbol{\varphi}_{k+1}\mathbf{P}_{\boldsymbol{\theta},k}\boldsymbol{\varphi}^T_{k+1}\right]^{-1} \tag{8}$$

$$\mathbf{S}_{k+1} = \left[\boldsymbol{\eta}^{*T}(\mathbf{I} - \boldsymbol{\varphi}_{k+1}\mathbf{K}_{\boldsymbol{\theta},k+1})\boldsymbol{\eta}^*\right]^{-1} \tag{9}$$

$$\mathbf{P}_{\theta,k} = (\mathbf{I} + \mathbf{K}_{\theta,k}\boldsymbol{\eta}^{*}\mathbf{S}_k\boldsymbol{\eta}^{*T}\boldsymbol{\varphi}_k)(\mathbf{I} - \mathbf{K}_{\theta,k}\boldsymbol{\varphi}_k)\mathbf{P}_{\theta,k-1} \tag{10}$$

where $\mathbf{K}_{\theta,k+1}$ is the (n×m) LSE gain matrix for $\hat{\theta}_{k+1}$. In Eq. (10), $\mathbf{K}_{\theta,k}$ and $\mathbf{S}_k$ are obtained, respectively, from Eqs. (8) and (9) by replacing k+1 by k. It can be shown easily that the recursive solution in Eqs. (6)-(10) reduces to the classical one when all the external excitations are known, i.e., $\boldsymbol{\eta}^* = \mathbf{0}$. The analytical solution derived in Eqs. (6)-(10) is referred to as the recursive LSE with unknown inputs (LSE-UI). For the numerical computation, Eq. (7) is used first to compute $\hat{\mathbf{f}}^*_{k+1|k+1}$ and then Eq. (6) is used to compute $\hat{\theta}_{k+1}$ (Yang *et al.* 2007a).

The recursive solution $\hat{\theta}_{k+1}$ in Eqs. (6)-(10) is derived based on the constant parametric vector θ_{k+1}. To identify time-varying parameters of the structures for detecting the damages, the adaptive tracking technique proposed by Yang and Lin (2004, 2005) can be used. Since the estimation error is reflected in the adaptation gain matrix $\mathbf{P}_{\theta,k}$ as shown by Eq. (10), $\mathbf{P}_{\theta,k}$ in Eq. (10) was proposed to be replaced by the following

$$\mathbf{P}_{\theta,k} = (\mathbf{I} + \mathbf{K}_{\theta,k}\boldsymbol{\eta}^{*}\mathbf{S}_k\boldsymbol{\eta}^{*T}\boldsymbol{\varphi}_k)(\mathbf{I} - \mathbf{K}_{\theta,k}\boldsymbol{\varphi}_k)(\boldsymbol{\Lambda}_k\mathbf{P}_{\theta,k-1}\boldsymbol{\Lambda}_k^T), \quad k = 1, 2, \ldots \tag{11}$$

In Eq. (11), Λ_{k+1} is a diagonal matrix, referred to as the adaptive factor matrix, with diagonal elements $\lambda_1(k+1)$, $\lambda_2(k+1)$,..., $\lambda_n(k+1)$, where $\lambda_j(k+1)$ is referred to as the adaptive factor for the estimated parameter $\theta_j(k+1)$ at $t = t_{k+1} = (k+1)\Delta t$. The determination of the adaptive factor matrix was discussed in (Yang and Lin 2005). The method presented in Eqs. (6)-(11) is referred to as the adaptive least-square estimation with unknown input (ALSE-UI), and it will be verified by experimental data later.

2.2 Extended Kalman filter with unknown inputs (EKF-UI)

In this approach, some acceleration responses and none or some of external excitations are measured, whereas the unknown displacement and velocity responses, the unknown parametric vector as well as the unmeasured excitations are to be estimated. Here, an extended state vector with a dimension of 2 m+n is introduced

$$\mathbf{Z}(t) = \{\mathbf{x}^T, \dot{\mathbf{x}}^T, \theta^T\}^T \tag{12}$$

and Eq. (1) is transformed into a nonlinear extended state equation, i.e.,

$$\dot{\mathbf{Z}}(t) = g(\mathbf{Z}, \mathbf{f}, \mathbf{f}^*, t) + \mathbf{w}(t) \tag{13}$$

in which $\mathbf{w}(t)$ = model noise (uncertainty) with zero mean and a covariance matrix $\mathbf{Q}(t)$. A nonlinear discrete equation for an observation vector (measured output) can be expressed as follows

$$\mathbf{y}_{k+1} = \mathbf{h}(\mathbf{Z}_{k+1}, \mathbf{f}_{k+1}, \mathbf{f}^*_{k+1}, k+1) + \mathbf{v}_{k+1} \tag{14}$$

in which $\mathbf{y}_{k+1}$ is a *l*-observation (measured) output vector at $t = (k+1)\Delta t$ i.e., $\mathbf{y}_{k+1} = \mathbf{y}(t = (k+1)\Delta t)$, $\mathbf{Z}_{k+1} = \mathbf{Z}(t = (k+1)\Delta t)$, $\mathbf{f}_{k+1} = \mathbf{f}(t = (k+1)\Delta t)$, and $\mathbf{f}^*_{k+1} = \mathbf{f}^*(t = (k+1)\Delta t)$. In Eq. (14), $\mathbf{v}_{k+1}$ is a measurement noise vector assumed to be a Gaussian white noise vector with zero mean and a covariance matrix $E[\mathbf{v}_k\mathbf{v}_j^T] = \mathbf{R}_k\delta_{kj}$ where δ_{kj} is the Kroneker delta.

Let $\hat{\mathbf{Z}}_{k+1|k+1}$ and $\hat{\mathbf{f}}^*_{k+1|k+1}$ be the estimates of $\mathbf{Z}_{k+1}$ and $\mathbf{f}^*_{k+1}$ predicted at $t = (k+1)\Delta t$. The goal is to determine the solutions for $\hat{\mathbf{Z}}_{k+1|k+1}$ and $\hat{\mathbf{f}}^*_{k+1|k+1}$ (for k=1,2,…) by minimizing an objective function J_{k+1} that is the sum square error as follows

$$J_{k+1} = \sum_{i=1}^{k+1} \boldsymbol{\Delta}_i^T \mathbf{R}_i^{-1} \boldsymbol{\Delta}_i \ ; \ \boldsymbol{\Delta}_i = \mathbf{y}_i - \mathbf{h}(\mathbf{Z}_i, \mathbf{f}_i, \mathbf{f}_i^*, i) \tag{15}$$

Based on the extended Kalman filter with unknown inputs (EKF-UI) approach (Yang *et al.* 2007b), the recursive solutions for the estimations $\hat{\mathbf{Z}}_{k+1|k+1}$ and $\hat{\mathbf{f}}^*_{k+1|k+1}$ (for k=1,2,…) are given in the following.

$$\hat{\mathbf{Z}}_{k+1|k+1} = \hat{\mathbf{Z}}_{k+1|k} + \mathbf{K}_{\mathbf{Z},k+1}\left[\mathbf{y}_{k+1} - \hat{\mathbf{h}}_{k+1|k} - \mathbf{D}^*_{k+1|k}(\hat{\mathbf{f}}^*_{k+1|k+1} - \hat{\mathbf{f}}^*_{k|k})\right] \tag{16}$$

$$\hat{\mathbf{f}}^*_{k+1|k+1} = \mathbf{S}_{k+1}\mathbf{D}^{*T}_{k+1|k}\mathbf{R}^{-1}_{k+1}\left(\mathbf{I} - \mathbf{H}_{k+1|k}\mathbf{K}_{\mathbf{Z},k+1}\right)\left(\mathbf{y}_{k+1} - \hat{\mathbf{h}}_{k+1|k} + \mathbf{D}^*_{k+1|k}\hat{\mathbf{f}}^*_{k|k}\right) \tag{17}$$

$$\hat{\mathbf{Z}}_{k+1|k} = \hat{\mathbf{Z}}_{k|k} + \int_{k\Delta t}^{(k+1)\Delta t} \mathbf{g}(\hat{\mathbf{Z}}_{t|k}, \mathbf{f}, \hat{\mathbf{f}}^*_{t|k}, t)\, dt \tag{18}$$

in which $\hat{\mathbf{h}}_{k+1|k} = \mathbf{h}(\hat{\mathbf{Z}}_{k+1|k}, \mathbf{f}_{k+1}, \hat{\mathbf{f}}^*_{k|k}, k+1)$, and

$$\mathbf{K}_{\mathbf{Z},k+1} = \mathbf{P}_{\mathbf{Z},k+1|k}\mathbf{H}^T_{k+1|k}\left[\mathbf{H}_{k+1|k}\mathbf{P}_{\mathbf{Z},k+1|k}\mathbf{H}^T_{k+1|k} + \mathbf{R}_{k+1}\right]^{-1} \tag{19}$$

$$\mathbf{S}_{k+1} = \left[\mathbf{D}^{*T}_{k+1|k}\mathbf{R}^{-1}_{k+1}(\mathbf{I} - \mathbf{H}_{k+1|k}\mathbf{K}_{\mathbf{Z},k+1})\mathbf{D}^*_{k+1|k}\right]^{-1} \tag{20}$$

$$\mathbf{P}_{\mathbf{Z},k+1|k} = \boldsymbol{\Phi}_{k+1,k}\,\mathbf{P}_{\mathbf{Z},k|k}\boldsymbol{\Phi}^T_{k+1,k} + \mathbf{Q}_{k+1} \tag{21}$$

$$\mathbf{P}_{\mathbf{Z},k|k} = \left(\mathbf{I} + \mathbf{K}_{\mathbf{Z},k}\mathbf{D}^*_{k|k-1}\mathbf{S}_k\mathbf{D}^{*T}_{k|k-1}\mathbf{R}^{-1}_k\mathbf{H}_{k|k-1}\right)\left(\mathbf{I} - \mathbf{K}_{\mathbf{Z},k}\mathbf{H}_{k|k-1}\right)\mathbf{P}_{\mathbf{Z},k|k-1} \tag{22}$$

where $\mathbf{Q}_{k+1}$ is the variance matrix of the model noise vector $\mathbf{w}(t)$ at $t = (k+1)\Delta t$, $\boldsymbol{\Phi}_{k+1,k}$ is the state transition matrix of the linearized system that is obtained from the linearization of Eq. (13).

In Eqs. (16)-(17), $\mathbf{H}_{k+1|k}$ and $\mathbf{D}^*_{k+1|k}$ are given by

$$\mathbf{H}_{k+1|k} = \left[\partial\mathbf{h}_{k+1}/\partial\mathbf{Z}_{k+1}\right]_{\mathbf{Z}_{k+1}=\hat{\mathbf{Z}}_{k+1|k},\,\mathbf{f}^*_{k+1}=\hat{\mathbf{f}}^*_{k|k}} \ ; \ \mathbf{D}^*_{k+1|k} = \left[\partial\mathbf{h}_{k+1}/\partial\mathbf{f}^*_{k+1}\right]_{\mathbf{Z}_{k+1}=\hat{\mathbf{Z}}_{k+1|k},\,\mathbf{f}^*_{k+1}=\hat{\mathbf{f}}^*_{k|k}} \tag{23}$$

The EKF-UI approach in Eqs. (16)-(23) (Yang *et al.* 2007b) can be used to identify the constant parameter vector $\boldsymbol{\theta}$. Again, the adaptive tracking technique proposed by Yang and Lin (2004, 2005) was implemented to identify time-varying parameters of the structures for detecting the damages. Since the estimation error is reflected in the adaptation gain matrix $\mathbf{P}_{\mathbf{Z},k+1|k}$ as shown by Eq. (21), $\mathbf{P}_{\mathbf{Z},k+1|k}$ in Eq. (21) was proposed to be replaced by the following (Yang *et al.* 2007b)

$$\mathbf{P}_{\mathbf{Z},k+1|k} = \boldsymbol{\Lambda}_{k+1}\left[\boldsymbol{\Phi}_{k+1,k}\mathbf{P}_{\mathbf{Z},k|k}\boldsymbol{\Phi}^T_{k+1,k}\right]\boldsymbol{\Lambda}^T_{k+1} + \mathbf{Q}_{k+1} \tag{24}$$

in which Λ_{k+1} is a (2m+n)×(2m+n) diagonal matrix, referred to as the adaptive factor matrix. The first 2m diagonal elements of Λ_{k+1} corresponding to $\mathbf{x}$ and $\dot{\mathbf{x}}$ are set to be 1.0, whereas the last n diagonal elements corresponding to unknown parameters are denoted by $\lambda_1(k+1)$, $\lambda_2(k+1)$,..., $\lambda_n(k+1)$. The determination of the adaptive factor matrix was discussed in (Yang *et al.* 2007b). The method presented in Eqs. (16)-(24) is referred to as the adaptive extended Kalman filter with unknown inputs (AEKF-UI), and it will be verified by experimental data later.

2.3 Sequential non-linear least-square estimation with unknown inputs and unknown outputs (SNLSE-UI-UO)

The LSE approach requires that the information for the acceleration and state vector at all degrees of freedom (DOFs) be available. Further, the dimension of the extended state vector $\mathbf{Z}$ in the EKF approach is large, so that the computational efforts for the damage detection is quite involved, in addition to possible convergence problem. To remove the drawbacks of LSE and EKF approaches for the damage identification, a new approach was proposed, referred to as the sequential non-linear least-square estimation with unknown inputs and unknown outputs (e.g., Yang and Huang 2007, Huang 2006). In this approach, some acceleration responses and none or some of excitation forces are measured. The acceleration vector $\ddot{\mathbf{x}}(t)=[\ddot{x}_1(t), \ddot{x}_2(t), \ldots, \ddot{x}_m(t)]^T$ in Eq.(1) is divided into two vectors, denoted by $\ddot{\mathbf{x}}^*(t)=[\ddot{x}_1^*(t), \ddot{x}_2^*(t), \ldots, \ddot{x}_s^*(t)]^T$ and $\ddot{\bar{\mathbf{x}}}(t)=[\ddot{\bar{x}}_1(t), \ddot{\bar{x}}_2(t), \ldots, \ddot{\bar{x}}_{m-s}(t)]^T$, in which $\ddot{x}_i^*(t)$ (i=1,2,…,s) and $\ddot{\bar{x}}_i(t)$ (i=1,2,…,m-s) are unknown (unmeasured) and known (measured) acceleration responses, respectively. The unknown quantities to be identified are the unknown parametric vector θ, the unmeasured excitation vector $\mathbf{f}^*$, the unmeasured acceleration response vector $\ddot{\mathbf{x}}^*$, and the state vector $\mathbf{X} = [\mathbf{x}^T, \dot{\mathbf{x}}^T]^T$, including the displacement and velocity vectors.

By adding the model uncertainty, $\varepsilon(t)$, Eq. (1), can be written in the following form

$$\varphi(\mathbf{X})\theta + \varepsilon = \bar{\eta}\bar{\mathbf{f}} + \mathbf{y} \tag{25}$$

in which $\mathbf{X}$ is the state vector defined above; $\varphi(\mathbf{X})$ is called the data matrix; $\mathbf{y}=(\eta\mathbf{f} - \bar{\mathbf{M}}\ddot{\bar{\mathbf{x}}})$ is known; $\bar{\mathbf{f}}=[\mathbf{f}^{*T} - \ddot{\mathbf{x}}^{*T}]^T$ is the unknown input-output vector consisting of unknown inputs $\mathbf{f}^*$ and unknown outputs $\ddot{\mathbf{x}}^*$; $\bar{\eta}=[\eta^* - \mathbf{M}^*]$ is a known matrix; and $\varepsilon(t)$ is a m-model noise vector.

Similar to the LSE-UI approach, one can define a (n+r+s)-extended unknown vector $\theta_{e,k+1}$ at t_{k+1} involving both θ_{k+1} and $\bar{\mathbf{f}}_{k+1}$. Instead of solving $\mathbf{X}_{k+1}$ and $\theta_{e,k+1}$ simultaneously, one can solve $\mathbf{X}_{k+1}$ and $\theta_{e,k+1}$ in two steps. The first step is to determine $\theta_{e,k+1}$ by assuming (or under the condition) that $\mathbf{X}_{k+1}$ is given, and the second step is to determine $\mathbf{X}_{k+1}$ through a nonlinear LSE approach, referred to as the sequential non-linear least-square estimation with unknown inputs and unknown outputs (SNLSE-UI-UO), as follows (Yang and Huang 2007).

Step I: Suppose the state vector $\mathbf{X}_{k+1}$ is known, the recursive solutions for $\hat{\theta}_{k+1}$ and $\hat{\bar{\mathbf{f}}}_{k+1|k+1}$, which are the estimates of θ_{k+1} and $\bar{\mathbf{f}}_{k+1}$ predicted at $t = (k+1)\Delta t$, have been derived based on the LSE-UI approach as follows

$$\hat{\boldsymbol{\theta}}_{k+1} = \hat{\boldsymbol{\theta}}_k + \mathbf{K}_{\boldsymbol{\theta},k+1}(\mathbf{X}_{k+1})[\mathbf{y}_{k+1} - \boldsymbol{\varphi}_{k+1}(\mathbf{X}_{k+1})\hat{\boldsymbol{\theta}}_k + \bar{\boldsymbol{\eta}}\hat{\bar{\mathbf{f}}}_{k+1|k+1}] \tag{26}$$

$$\hat{\bar{\mathbf{f}}}_{k+1|k+1} = -\mathbf{S}_{k+1}(\mathbf{X}_{k+1})\bar{\boldsymbol{\eta}}^T[\mathbf{I} - \boldsymbol{\varphi}_{k+1}(\mathbf{X}_{k+1})\mathbf{K}_{\boldsymbol{\theta},k+1}(\mathbf{X}_{k+1})][\mathbf{y}_{k+1} - \boldsymbol{\varphi}_{k+1}(\mathbf{X}_{k+1})\hat{\boldsymbol{\theta}}_k] \tag{27}$$

$$\mathbf{K}_{\boldsymbol{\theta},k+1}(\mathbf{X}_{k+1}) = \mathbf{P}_{\boldsymbol{\theta},k}\boldsymbol{\varphi}_{k+1}^T(\mathbf{X}_{k+1})[\mathbf{I} + \boldsymbol{\varphi}_{k+1}(\mathbf{X}_{k+1})\mathbf{P}_{\boldsymbol{\theta},k}\boldsymbol{\varphi}_{k+1}^T(\mathbf{X}_{k+1})]^{-1} \tag{28}$$

$$\mathbf{S}_{k+1}(\mathbf{X}_{k+1}) = \{\bar{\boldsymbol{\eta}}^T[\mathbf{I} - \boldsymbol{\varphi}_{k+1}(\mathbf{X}_{k+1})\mathbf{K}_{\boldsymbol{\theta},k+1}(\mathbf{X}_{k+1})]\bar{\boldsymbol{\eta}}\}^{-1} \tag{29}$$

$$\mathbf{P}_{\boldsymbol{\theta},k} = [\mathbf{I} + \mathbf{K}_{\boldsymbol{\theta},k}(\mathbf{X}_k)\bar{\boldsymbol{\eta}}\mathbf{S}_k(\mathbf{X}_k)\bar{\boldsymbol{\eta}}^T\boldsymbol{\varphi}_k(\mathbf{X}_k)][\mathbf{P}_{\boldsymbol{\theta},k-1} - \mathbf{K}_{\boldsymbol{\theta},k}(\mathbf{X}_k)\boldsymbol{\varphi}_k(\mathbf{X}_k)\mathbf{P}_{\boldsymbol{\theta},k-1}] \tag{30}$$

in which $\mathbf{K}_{\theta,k+1}(\mathbf{X}_{k+1})$, $\varphi_{k+1}(\mathbf{X}_{k+1})$ and $\mathbf{P}_{\theta,k}$ are defined similarly in the LSE-UI approach, except that the former two matrices are functions of the state vector $\mathbf{X}_{k+1}$.

Step II: As observed from Eqs. (26)-(30), $\hat{\theta}_{k+1}$ is a function of the unknown state vector $\mathbf{X}_{k+1}$, i.e., $\hat{\theta}_{k+1} = \hat{\theta}_{k+1}(\mathbf{X}_{k+1})$. The estimate $\hat{\mathbf{X}}_{k+1|k+1}$ of $\mathbf{X}_{k+1}$ was obtained by the following recursive solution (Yang and Huang 2007).

$$\hat{\mathbf{X}}_{k+1|k+1} = \hat{\mathbf{X}}_{k+1|k} + \overline{\mathbf{K}}_{k+1}[\mathbf{y}_{k+1} - \hat{\mathbf{y}}_{k+1}(\hat{\mathbf{X}}_{k+1|k})] \tag{31}$$

where $\hat{\mathbf{y}}_{k+1}(\hat{\mathbf{X}}_{k+1|k}) = \boldsymbol{\varphi}_{k+1}(\hat{\mathbf{X}}_{k+1|k})\hat{\boldsymbol{\theta}}_{k+1}$, and

$$\hat{\mathbf{X}}_{k+1|k} = \mathbf{\Phi}_{k+1,k}\hat{\mathbf{X}}_{k|k} + \mathbf{B}_1\ddot{\mathbf{x}}_k + \mathbf{B}_2\ddot{\mathbf{x}}_{k+1} \tag{32}$$

In Eqs. (31) and (32), $\mathbf{\Phi}_{k+1,k}$ is the transition matrix for the state vector from k to k+1, and $\mathbf{B}_1$, $\mathbf{B}_2$ and $\overline{\mathbf{K}}_{k+1}$ are appropriate matrices (see Yang and Huang 2007).

The recursive solution for $\hat{\theta}_{k+1}$ in Eqs. (26)-(30) was derived based on the constant parametric vector θ_{k+1}. Similarly, the adaptive tracking technique proposed in (Yang and Lin 2005) can be implemented to identify time-varying parameters of the structures for detecting the damages. Again, the modification is reflected by the $\mathbf{P}_{\theta,k}$ matrix in Eq. (30), i.e., $\mathbf{P}_{\theta,k} \rightarrow \Lambda_{k+1}\mathbf{P}_{\theta,k}\Lambda_{k+1}$, where Λ_{k+1} is the (n×n) adaptive factor matrix (see Yang and Huang 2007). This approach is referred to as the adaptive sequential non-linear least-square estimation with unknown inputs and unknown outputs (ASNLSE-UI-UO), and it will be verified by experimental data later.

2.4 Quadratic sum-squares error with unknown inputs (QSSE-UI)

A newly proposed approach (Huang 2006, Huang *et al.* 2010), referred to as the quadratic sum-squares error with unknown inputs (QSSE-UI), can also be used for the on-line damage identification with limited measurements of acceleration responses and external excitations. In this approach, the state vector, $\mathbf{X} = \{\mathbf{x}^T, \dot{\mathbf{x}}^T\}^T$, is considered as an implicit function of the unknown parametric vector θ, i.e., $\mathbf{X} = \mathbf{X}(\theta)$.

The nonlinear discrete equation at $t = (k+1)\Delta t$ for an observation vector (measured output) can be expressed as

$$\mathbf{y}_{k+1} = \mathbf{h}[\mathbf{X}_{k+1}(\boldsymbol{\theta}_{k+1}), \boldsymbol{\theta}_{k+1}, \mathbf{f}^*_{k+1}, \mathbf{f}_{k+1}] + \mathbf{v}_{k+1} \tag{33}$$

in which $\mathbf{y}_{k+1}$, $\mathbf{f}_{k+1}$ $\mathbf{f}^*_{k+1}$ and $\mathbf{v}_{k+1}$ have the same definition as that given in Eq. (14) for the EKF-UI approach, $\mathbf{X}_{k+1}(\theta_{k+1})$ is an implicit function of the unknown parametric vector θ_{k+1}. Given the measured response data $\mathbf{y}_{k+1}$ and some (or none) measured external excitation $\mathbf{f}_{k+1}$, the goal is to estimate the unknown parametric vector θ_{k+1} and the unmeasured input $\mathbf{f}^*_{k+1}$ directly. The approach herein is to determine θ_{k+1} and $\mathbf{f}^*_{k+1}$ by minimizing the sum-squares error between the measured response data $\mathbf{y}_{k+1}$ and the theoretical expression of the measured quantities similar to that given by Eq. (15). Further, since $\mathbf{h}[\mathbf{X}_{k+1}(\theta_{k+1}), \theta_{k+1}, \mathbf{f}^*_{k+1}, \mathbf{f}_{k+1}]$ is a nonlinear function of the unknown vectors θ_{k+1} and $\mathbf{f}^*_{k+1}$, it will be linearized as a linear function of θ_{k+1} and $\mathbf{f}^*_{k+1}$ through a Taylor's series expansion. Then, the sum-square error becomes a quadratic function of unknown vectors θ_{k+1} and $\mathbf{f}^*_{k+1}$, and hence the solution can be obtained.

Define an extended unknown vector $\theta_{e,k+1}$ and an extended matrix $\mathbf{H}_{e,k+1}$ at $t = (k+1)\Delta t$, i.e.,

$$\boldsymbol{\theta}_{e,k+1} = \begin{bmatrix} \boldsymbol{\theta}_{k+1} \\ \hdashline \mathbf{f}^*_{k+1} \end{bmatrix}; \quad \mathbf{H}_{e,k+1} = [\mathbf{H}_{k+1} \;\vdots\; \mathbf{D}_{k+1}] \tag{34}$$

where $\mathbf{H}_{k+1}$ and $\mathbf{D}^*_{k+1}$ are given by

$$\mathbf{H}_{k+1} = \left[\partial\,\mathbf{h}_{k+1}/\partial\,\boldsymbol{\theta}_{k+1}\right]_{\boldsymbol{\theta}_{k+1}=\hat{\boldsymbol{\theta}}_k,\,\mathbf{f}^*_{k+1}=\hat{\mathbf{f}}^*_{k|k}}\ ;\quad \mathbf{D}^*_{k+1} = \left[\partial\,\mathbf{h}_{k+1}/\partial\,\mathbf{f}^*_{k+1}\right]_{\boldsymbol{\theta}_{k+1}=\hat{\boldsymbol{\theta}}_k,\,\mathbf{f}^*_{k+1}=\hat{\mathbf{f}}^*_{k|k}} \tag{35}$$

The recursive solutions for the estimations $\hat{\theta}_{k+1}$ and $\hat{\mathbf{f}}^*_{k+1|k+1}$ of θ_{k+1} and $\mathbf{f}^*_{k+1}$, respectively, at $t=(k+1)\Delta t$ can be derived using a similar procedure as that used in the LSE-UI approach (see Huang 2006, Huang *et al.* 2010); with the results

$$\hat{\boldsymbol{\theta}}_{k+1} = \hat{\boldsymbol{\theta}}_k + \mathbf{K}_{\boldsymbol{\theta},k+1}[\mathbf{y}_{k+1} - \hat{\mathbf{h}}_{k+1} - \mathbf{D}_{k+1}(\hat{\mathbf{f}}^*_{k+1|k+1} - \hat{\mathbf{f}}^*_{k|k})] \tag{36}$$

$$\hat{\mathbf{f}}^*_{k+1|k+1} = \mathbf{S}_{k+1}\mathbf{D}^T_{k+1}\mathbf{R}^{-1}_{k+1}(\mathbf{I} - \mathbf{H}_{k+1}\mathbf{K}_{\boldsymbol{\theta},k+1})(\mathbf{y}_{k+1} - \hat{\mathbf{h}}_{k+1} + \mathbf{D}_{k+1}\hat{\mathbf{f}}^*_{k|k}) \tag{37}$$

where

$$\mathbf{K}_{\boldsymbol{\theta},k+1} = \mathbf{P}_{\boldsymbol{\theta},k}\mathbf{H}^T_{k+1}(\mathbf{R}_{k+1} + \mathbf{H}_{k+1}\mathbf{P}_{\boldsymbol{\theta},k}\mathbf{H}^T_{k+1})^{-1} \tag{38}$$

$$\mathbf{S}_{k+1} = \left[\mathbf{D}^T_{k+1}\mathbf{R}^{-1}_{k+1}(\mathbf{I} - \mathbf{H}_{k+1}\mathbf{K}_{\boldsymbol{\theta},k+1})\mathbf{D}_{k+1}\right]^{-1} \tag{39}$$

$$\mathbf{P}_{\boldsymbol{\theta},k} = \left(\mathbf{I} + \mathbf{K}_{\boldsymbol{\theta},k}\mathbf{D}_k\mathbf{S}_k\mathbf{D}^T_k\mathbf{R}^{-1}_k\mathbf{H}_k\right)\left(\mathbf{I} - \mathbf{K}_{\boldsymbol{\theta},k}\mathbf{H}_k\right)\mathbf{P}_{\boldsymbol{\theta},k-1} \tag{40}$$

in which $\mathbf{K}_{\theta,k+1}$ is the $(n\times l)$ gain matrix for $\hat{\theta}_{k+1}$, and $\mathbf{R}_{k+1}$ is the variance matrix of the measurement noises at $t=(k+1)\Delta t$. In Eq. (40), $\mathbf{K}_{\theta,k}$ and $\mathbf{S}_k$ are obtained, respectively, from Eqs. (38) and (39) by replacing k+1 by k.

For the numerical computation, $\hat{\mathbf{h}}_{k+1}=\mathbf{h}(\hat{\mathbf{X}}_{k+1|k}, \hat{\theta}_k, \hat{\mathbf{f}}^*_{k|k}, \mathbf{f}_{k+1})$ is first obtained, in which $\hat{\mathbf{X}}_{k+1|k}$ is the estimate of the state vector $\mathbf{X}(t)$ at $t=(k+1)\Delta t$ based on $\theta=\hat{\theta}_k$ and $\mathbf{f}^*=\hat{\mathbf{f}}^*_{k|k}$, i.e.,

$$\hat{\mathbf{X}}_{k+1|k} = \hat{\mathbf{X}}_{k|k} + \int_{k\Delta t}^{(k+1)\Delta t}\mathbf{g}(\hat{\mathbf{X}}_{t|k}, \hat{\boldsymbol{\theta}}_k, \hat{\mathbf{f}}^*_{k|k}, \mathbf{f})\,dt \tag{41}$$

Consequently, Eq.(37) is used to compute $\hat{\mathbf{f}}^*_{k+1|k+1}$, and then Eq. (36) is used to compute $\hat{\theta}_{k+1}$. In the original papers for AQSSE and AQSSE-UI (Yang *et al.* 2009, Huang *et al.* 2010), the state vector $\hat{\mathbf{X}}_{k+1|k}$ is further up-dated using a Kalman filter. Based on our extensive numerical evaluations, this procedure is usually not necessary.

Similar to the ALSE-UI, AEKF-UI and ASNLSE-UI-UO approaches, the adaptive tracking technique proposed by Yang and Lin (2004, 2005) can be used to identify the parametric variations due to structural damages. Again, the modification of the recursive solution is reflected by the $\mathbf{P}_{\theta,k}$ matrix, i.e., $\mathbf{P}_{\theta,k}\rightarrow\Lambda_{k+1}\mathbf{P}_{\theta,k}\Lambda_{k+1}$, in which Λ_{k+1} is the $(n\times n)$ adaptive factor matrix (Huang 2006, Huang *et al.* 2010). This approach is referred to as the adaptive quadratic sum-squares error with unknown inputs (AQSSE-UI), and it will be verified by experimental data later.

3. Experimental verifications

Experimental tests for the damage tracking of structures have been conducted and experimental data for different damage scenarios have been available (Zhou *et al.* 2008). These experimental data will be used to verify the capability and accuracy of the ALSE-UI, AEKF-UI, ASNLSE-UI-UO and AQSSE-UI approaches for tracking the structural damage. The experiments conducted in Zhou *et al.* (2008) are described briefly in the following. A 400 mm by 300 mm scaled 3-story building model, as shown in Fig. 1(a), was used in the experiment. The height of the building model is 885 mm and the total weight is 75.4 kg. The mass of each floor are $m_1 = m_2 = 25.1$ kg, $m_3 = 24.8$ kg, and the first three natural frequencies are: 3.38 Hz, 9.47 Hz and 23.68 Hz, respectively. Based on the discretized 3-DOF shear-beam model, the stiffness of each story is obtained as 55.5 kN/m using the finite-element estimate, referred to as the referenced values. A white noise excitation force is applied to the top floor in the 400 mm direction using an exciter equipped with a force sensor (PCB2008C03). Each floor is installed with one acceleration sensor and one displacement sensor to measure the floor responses.

The damage in a story unit is assumed to be reflected by the reduction of its stiffness. To simulate the reduction of stiffness in a selected story, say ith story, an innovative stiffness element device (SED) with an effective stiffness of K_{hi} is installed in the ith story, so that the stiffness of the ith story is increased by K_{hi}. During the experimental test, the effective stiffness of the SED is reduced to zero to simulate the reduction of the stiffness in the ith story. The SED consists of a hydraulic cylinder-piston (HCP) with a valve on each side of the piston as shown in Fig. 1(b), which is connected in series to a bracing system shown schematically in Fig. 1(c). With the valves closed, the HCP is filled with air at an air pressure of P_0 that is proportional to the stiffness of the HCP.

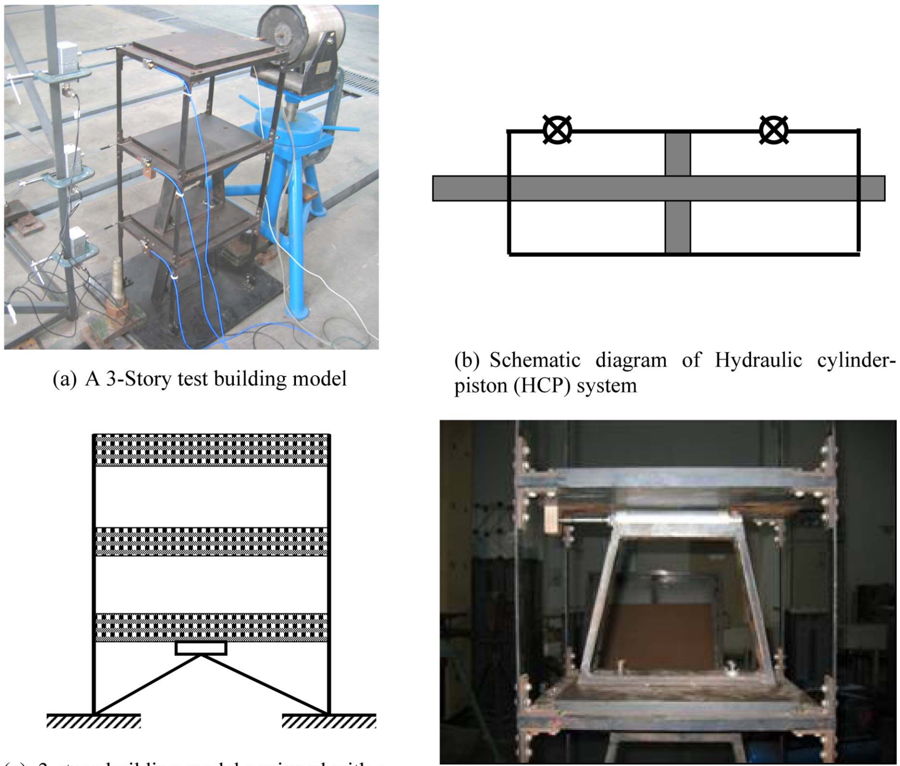

(a) A 3-Story test building model

(b) Schematic diagram of Hydraulic cylinder-piston (HCP) system

(c) 3-story building model equipped with a stiffness element device (SED) in first story

(d) Experimental set-up of SED in second story

Fig. 1 Experimental set-up

Hence, the stiffness of the HCP can be regulated by adjusting the air pressure P_0. Since the stiffness of the bracing is much bigger than that of the HCP and since both the HCP and the bracing are connected in series, the effective stiffness of the SED is approximately equal to that of the HCP. The effective stiffness of SED can be reduced to zero by opening both valves in HCP during the experimental test. This innovative stiffness element device (SED) is motivated by the so-called resetable semi-active stiffness dampers (Yang *et al*. 2000, 2007c). Detailed experimental tests were described in Zhou *et al.* (2008).

The acceleration and displacement responses of all floors, (a_1, a_2, a_3) and (d_1, d_2, d_3), as well as the white noise excitation, f(t), were measured in all tests. The sampling frequency of all measurements is 200 Hz. Unknown quantities to be estimated are the stiffness parameters of all stories k_i (i=1, 2, 3).

3.1 Damage Case 1: single damage in first story

In this test, a stiffness element device (SED), consisting of a hydraulic cylinder-piston (HCP) and a bracing system, is installed in the first story as shown in Fig. 1(c). The HCP is filled with air at an air pressure of 0.4 MPa. From the experimental test of the HCP, a gas pressure at P_0= 0.4 MPa results in an effective stiffness of 6.0 kN/m for the SED. Hence, the stiffness of the first story is k_1 = 55.5 kN/m + 6.0 kN/m = 61.5 kN/m, whereas the stiffness of other two stories is $k_2 = k_3 = 55.5$ kN/m. During the test, both valves of the HCP were closed at the beginning and were open simultaneously at t = 25 seconds, so that the stiffness in the first story reduces abruptly from 61.5 kN/m to 55.5 kN/m at t = 25 seconds.

3.2 Damage Case 2: single damage in second story

Now the stiffness element device (SED) is installed in the second story as shown in Fig. 1(d), and the HCP is filled with air at an air pressure of 0.7 MPa that results in an effective stiffness of 10.5 kN/m for SED. Hence, the stiffness of the second story is k_2 = 55.5 kN/m + 10.5 kN/m = 66 kN/m, whereas the stiffness of other two stories is $k_1 = k_3 = 55.5$ kN/m. The total weight of the SED is 5.1 kg, which should be added to the first floor. Thus, the mass of the first floor is increased to 30.2 kg, whereas the mass of other floors are still $m_2 = 25.1$ kg and $m_3 = 24.8$ kg. During the test, both valves of the HCP were open simultaneously at t = 18 seconds, so that the stiffness in the second story reduces abruptly from 66 kN/m to 55.5 kN/m at t = 18 seconds.

3.3 Damage Case 3: damages in first and second stories

In this case, one stiffness element device (SED) is installed in the first story and another SED is installed in the second story. Both HCPs are filled with air at an air pressure of 0.7 MPa that results in an effective stiffness of 10.5 kN/m for each SED. Hence, the stiffness of the first and second stories are 66 kN/m, whereas the stiffness of the third story is 55.5 kN/m. Due to the added masses of the SED devices, the mass of each floor are: $m_1 = 30.2$ kg, $m_2 = 25.1$ kg and $m_3 = 24.8$ kg. During the test, both valves of the SED in the second story were open at t = 27 seconds, so that the stiffness of the second story reduces abruptly from 66 kN/m to 55.5 kN/m at t = 27 seconds. Then, the valves of the SED in the first story were open at t = 35 seconds, so that the stiffness of the first story reduces abruptly from 66 kN/m to 55.5 kN/m.

4. Results and discussion

In this study, the test model is considered as a 3-DOF shear-beam building structure, and the state equation of motion can be written analytically. Different damage tracking techniques are compared numerically for two different scenarios: (i) the external excitation is measured (known input), and (ii) the external excitation is not measured (unknown input).

4.1 Known inputs

Suppose the acceleration responses and the white noise excitations are measured, as shown in Fig. 2, for all the Damage Cases 1, 2 and 3 described above. In order to start the recursive solutions, some initial values have been assumed for each approach, as listed in Table 1. Based on the measured data in Fig. 2, the identified stiffness of all stories for Damage Cases 1-3 are presented in Figs. 3-5 as solid curves for each damage tracking technique including: (a) ALSE, (b) AEKF, (c) ASNLSE and (d) AQSSE. The dashed curves in Figs. 3-5 for comparison are the referenced values based on the finite-element estimation. The identified results for the stiffness of all stories for all cases are also summarized in Table 2 for comparison.

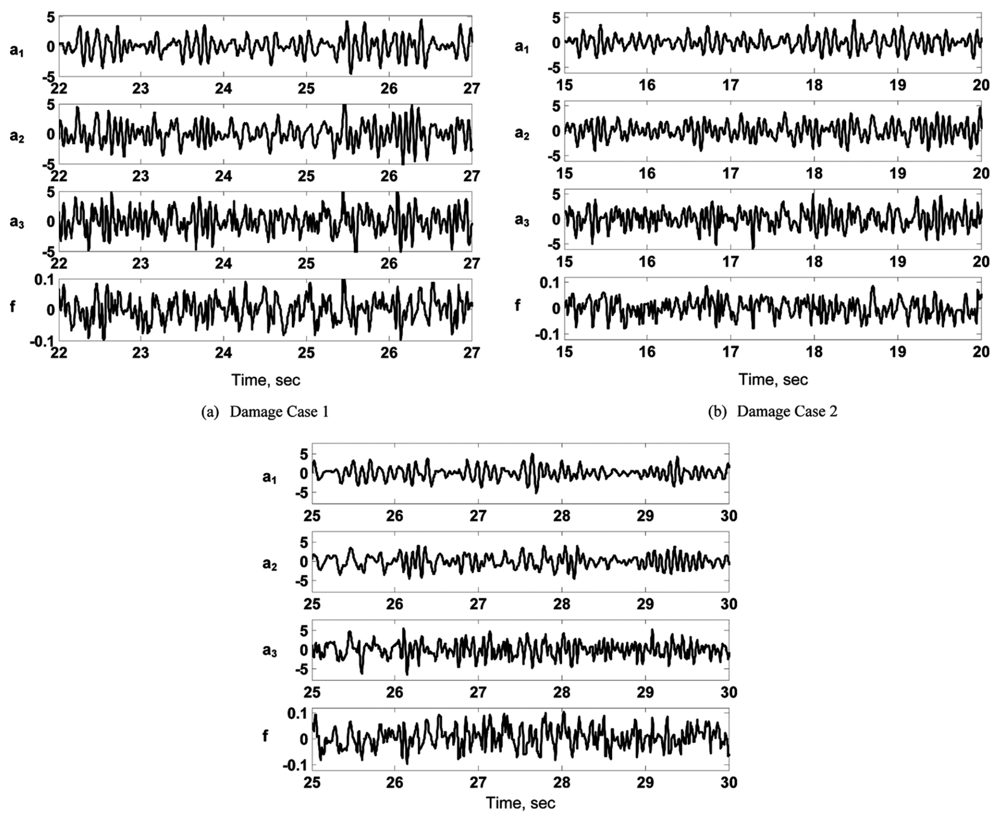

Fig. 2 Measured acceleration responses and white noise excitation force for 3 Damage Cases; a_i in m/s^2 and f in kN

Table 1 Initial values for each approach (known input)

	ALSE	AEKF	ASNLSE	AQSSE
State variables	zero	zero	zero	zero
$c_{i,0}$ (kN·s/m)	0.1	0.1	0.1	0.1
$k_{i,0}$ (kN/m)	100	40	100	10
$\mathbf{P}_0$, $\mathbf{P}_{0\|0}$	$\mathbf{P}_0 = 10^4\mathbf{I}_6$	$\mathbf{P}_{0\|0} = \mathrm{diag}[\mathbf{I}_9\ 10^2\,\mathbf{I}_3]$	$\mathbf{P}_0 = 10^4\mathbf{I}_6$, $\mathbf{P}_{0\|0} = \mathbf{I}_6]$	$\mathbf{P}_0 = \mathrm{diag}[\mathbf{I}_3\ 10^3\,\mathbf{I}_3]$
$\mathbf{Q}_0$	NA	$\mathbf{Q}_0 = 10^{-9}\,\mathbf{I}_{12}$	NA	NA
$\mathbf{R}_k = \mathbf{R}$	NA	$\mathbf{I}_3$	NA	$\mathbf{I}_3$
$\mathbf{X}_{\theta,0}$	NA	NA	NA	zero

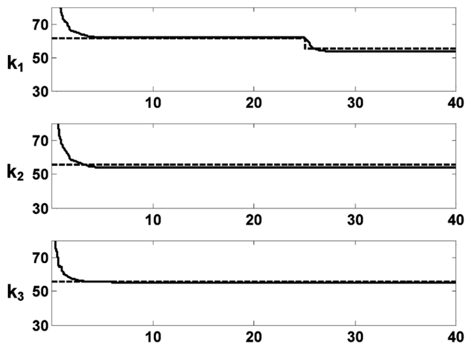

(a) ALSE

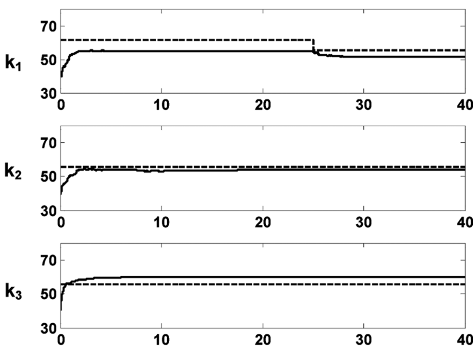

(b) AEKF

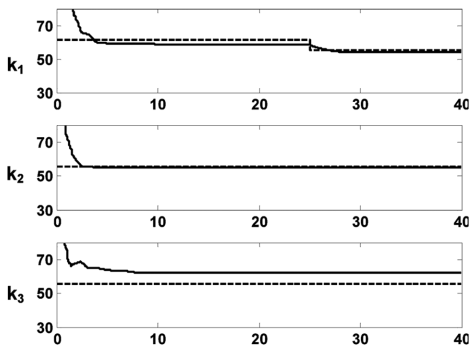

(c) ASNLSE

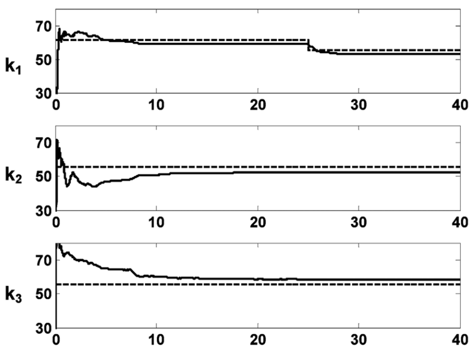

(d) AQSSE

Fig. 3 Identified stiffness parameters (k_i in kN/m) for Damage Case 1 using different approaches with known input; (a) ALSE, (b) AEKF, (c) ASNLSE and (d) AQSSE

It is observed from Figs. 3-5 and Table 2 that the identified stiffness based on each approach is quite reasonable in comparison with that of the referenced values, and that all the approaches under investigation are capable of tracking both the stiffness parameters and their variations due to damage. However, for the application of ALSE approach, all the responses, including acceleration, velocity and displacement have to be available. In this study, both acceleration and displacement responses are directly measured from the experiments, while the velocity responses are obtained by

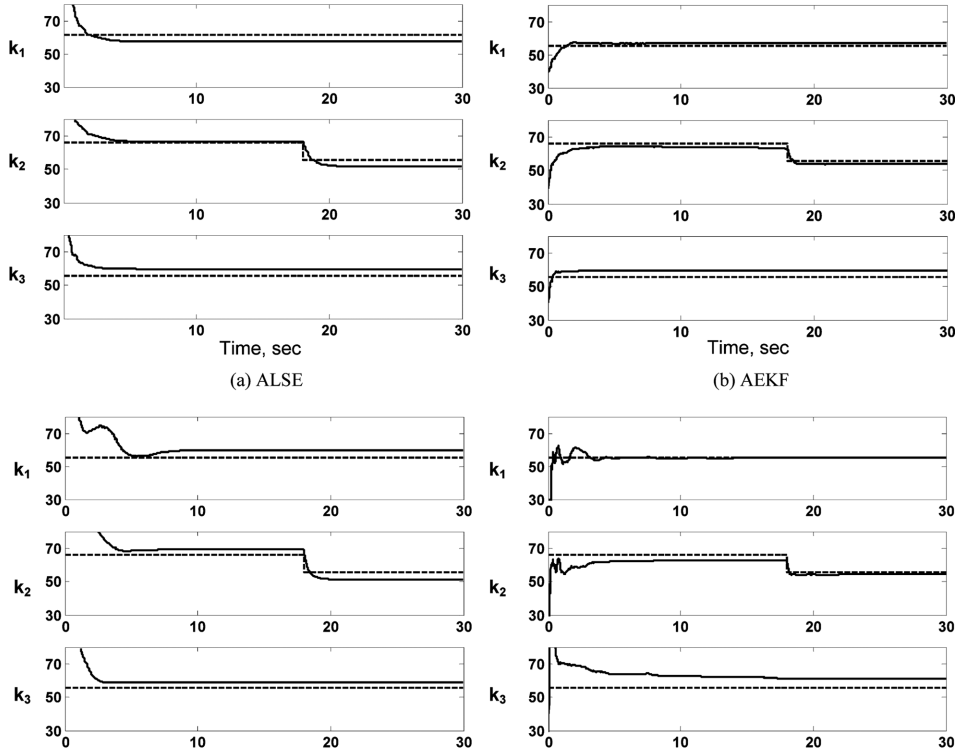

(a) ALSE (b) AEKF

(c) ASNLSE (d) AQSSE

Fig. 4 Identified stiffness parameters (k_i in kN/m) for Damage Case 2 using different approaches with known input; (a) ALSE, (b) AEKF, (c) ASNLSE and (d) AQSSE

differentiation of the displacements. In practice, only acceleration responses are usually measured, whereas the velocity responses can be obtained through a single numerical integration. For the displacement response, however, a double numerical integration from the acceleration response results in a significant numerical drift that is also magnified seriously when damages occur (Yang and Lin 2005). Nevertheless, such a numerical drift can be removed using special approaches (see Yang and Lin 2005).

With only the measurements of acceleration responses, the AEKF, ASNLSE and AQSSE approaches can be used for the online system identification and damage identification, where both the constant n-parametric vector θ and the 2 m-state vector $\mathbf{X}$ are treated as unknown quantities to be estimated. However, in the AEKF approach, an unknown (n+2m) extended state vector $\mathbf{Z}$, consisting of θ and $\mathbf{X}$, is introduced, and the resulting state equation for $\mathbf{Z}$ is highly nonlinear. The nonlinear equation is then linearized and the Kalman filter approach is applied. Unfortunately, some poles corresponding to the unknown θ of the linearized state equation lie on the imaginary axis, such that the solutions (estimates) may easily become unstable. Further, due to the linearization, the solutions may not converge if the initial guesses of the parametric values are outside the region of convergence. Likewise, the dimension (n+2 m) of the extended state vector $\mathbf{Z}$ is quite large, especially for large and complex structures, and hence the computational efforts required for estimating $\mathbf{Z}$ is quite involved.

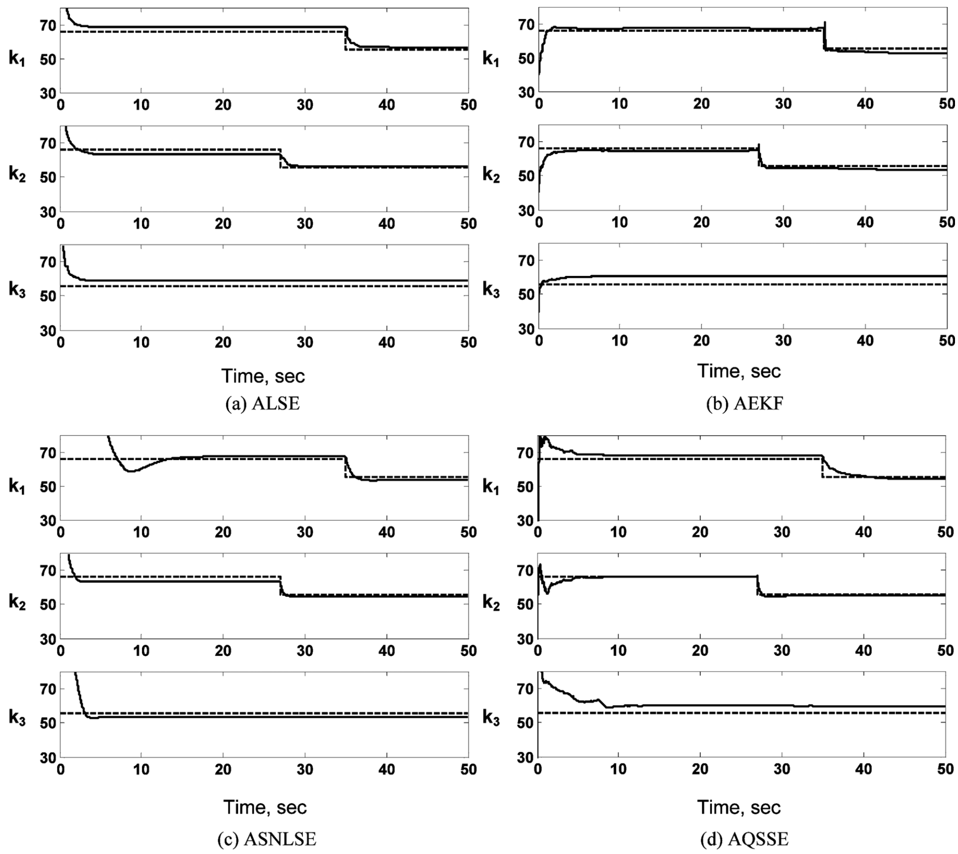

Fig. 5 Identified stiffness parameters (k_i in kN/m) for Damage Case 3 using different approaches with known input; (a) ALSE, (b) AEKF, (c) ASNLSE and (d) AQSSE

Table 2.1 Identified stiffness parameters before damage for all Damage Cases (known input)

		ALSE		AEKF		ASNLSE		AQSSE	
Case 1	Ref. values	Predicted	Difference (%)	Predicted	Difference (%)	Predicted	Difference (%)	Predicted	Difference (%)
k1	61.5	61.87	0.59	54.84	10.83	58.61	4.70	59.14	3.84
k2	55.5	53.91	2.87	53.85	2.97	55.14	0.65	52.21	5.92
k3	55.5	55.27	0.41	59.73	7.62	62.09	11.87	58.46	5.34
Case 2	Ref. values	Predicted	Difference (%)	Predicted	Difference (%)	Predicted	Difference (%)	Predicted	Difference (%)
k1	55.5	57.45	3.51	56.82	2.38	59.85	7.84	55.05	0.80
k2	66	66.67	1.02	63.95	3.10	69.10	4.70	62.83	4.81
k3	55.5	59.66	7.50	59.67	7.50	59.06	6.42	61.14	10.15
Case 3	Ref. values	Predicted	Difference (%)	Predicted	Difference (%)	Predicted	Difference (%)	Predicted	Difference (%)
k1	66	68.65	4.02	67.60	2.42	67.32	2.00	67.88	2.85
k2	66	63.23	4.20	64.56	2.18	63.51	3.77	66.12	0.18
k3	55.5	58.76	5.87	60.43	8.88	53.52	3.56	60.08	8.24

Table 2.2 Identified stiffness parameters after damage for all Damage Cases (known input)

		ALSE		AEKF		ASNLSE		AQSSE	
Case 1	Ref. values	Predicted	Difference (%)	Predicted	Difference (%)	Predicted	Difference (%)	Predicted	Difference (%)
k1	55.5	53.36	3.86	51.55	7.11	53.90	2.89	53.10	4.33
k2	55.5	53.91	2.87	53.94	2.81	55.14	0.65	52.21	5.92
k3	55.5	55.27	0.41	59.73	7.62	62.09	11.87	58.46	5.34
Case 2	Ref. values	Predicted	Difference (%)	Predicted	Difference (%)	Predicted	Difference (%)	Predicted	Difference (%)
k1	55.5	57.45	3.51	56.77	2.29	59.85	7.84	55.05	0.80
k2	55.5	51.69	6.86	53.71	3.22	51.23	7.69	54.28	2.19
k3	55.5	59.66	7.50	59.67	7.51	59.06	6.42	61.14	10.15
Case 3	Ref. values	Predicted	Difference (%)	Predicted	Difference (%)	Predicted	Difference (%)	Predicted	Difference (%)
k1	55.5	56.66	2.10	52.71	5.02	53.72	3.21	53.90	2.88
k2	55.5	55.86	0.65	53.29	3.98	54.54	1.74	54.89	1.10
k3	55.5	58.76	5.87	60.44	8.90	53.52	3.56	59.49	7.19

As for the ASNLSE and AQSSE approaches, the unknown parametric vector θ and the unknown state vector $\mathbf{X}$ are estimated sequentially in two steps. In the ASNLSE approach, the parametric vector θ is obtained first by minimizing an objective function, and then the state vector $\mathbf{X}$ is estimated, while in the AQSSE approach, the state equation of motion is considered as a constraint, and the unknown parametric vector θ is estimated directly. Therefore, the advantage of these two approaches is that it avoids inversion of large matrices as required in the AEKF approach and significantly reduces the computational efforts.

Hence, among the four approaches investigated in this study, the ASNLSE and AQSSE approaches are more suitable for damage identification of structures, in terms of accuracy, convergence and efficiency. Further, it is observed from Figs. 3-5 that the rate of convergence for identified results using the ASNLSE approach is slightly slower in comparison with other three approaches. This is be due to the sensitivity of the method with respect to the sampling frequency, since the estimation of state vectors using Newmark-β method produces more accurate results with a higher sampling frequency. Hence, the convergence of the solutions is expected to be faster for the ASNLSE approach as the sampling frequency increases.

4.2 Unknown inputs

Suppose only the acceleration responses are measured for Damage Cases 1-3, i.e., the measured excitation is not used in the prediction of unknown parameters. The initial values used to start the recursive solutions for each approach are listed in Table 3. Based only on the measured acceleration responses and different damage tracking techniques, the identified stiffness of all stories for Damage Cases 1-3 are presented in Figs. 6-8 as solid curves, whereas the dashed curves shown in these figures for comparison are the referenced values based on the finite-element estimation. The identified results for the stiffness of all stories for all cases are also summarized in Table 4 for comparison.

Table 3 Initial values for each approach (unknown input)

	ALSE-UI	AEKF-UI	ASNLSE-UI-UO	AQSSE-UI
State variables	zero	zero	zero	zero
$c_{i,0}$ (kN·s/m)	0.1	0.1	0.1	0.1
$k_{i,0}$ (kN/m)	100	40	80	40
$\mathbf{P}_0$, $\mathbf{P}_{0\|0}$	$\mathbf{P}_0 = 10^4\mathbf{I}_6$	$\mathbf{P}_{0\|0} = \mathrm{diag}[\mathbf{I}_9\ 10^4\ \mathbf{I}_3]$	$\mathbf{P}_0 = 10^3\mathbf{I}_6$, $\mathbf{P}_{0\|0} = \mathbf{I}_6$	$\mathbf{P}_0 = \mathrm{diag}[10\mathbf{I}_3\ 10^3\ \mathbf{I}_3]$
$\mathbf{Q}_0$	NA	$\mathbf{Q}_0 = 10^{-9}\ \mathbf{I}_{12}$	NA	NA
$\mathbf{R}_k = \mathbf{R}$	NA	$\mathbf{I}_3$	NA	$\mathbf{I}_3$
$\mathbf{X}_{\theta,0}$	NA	NA	NA	zero

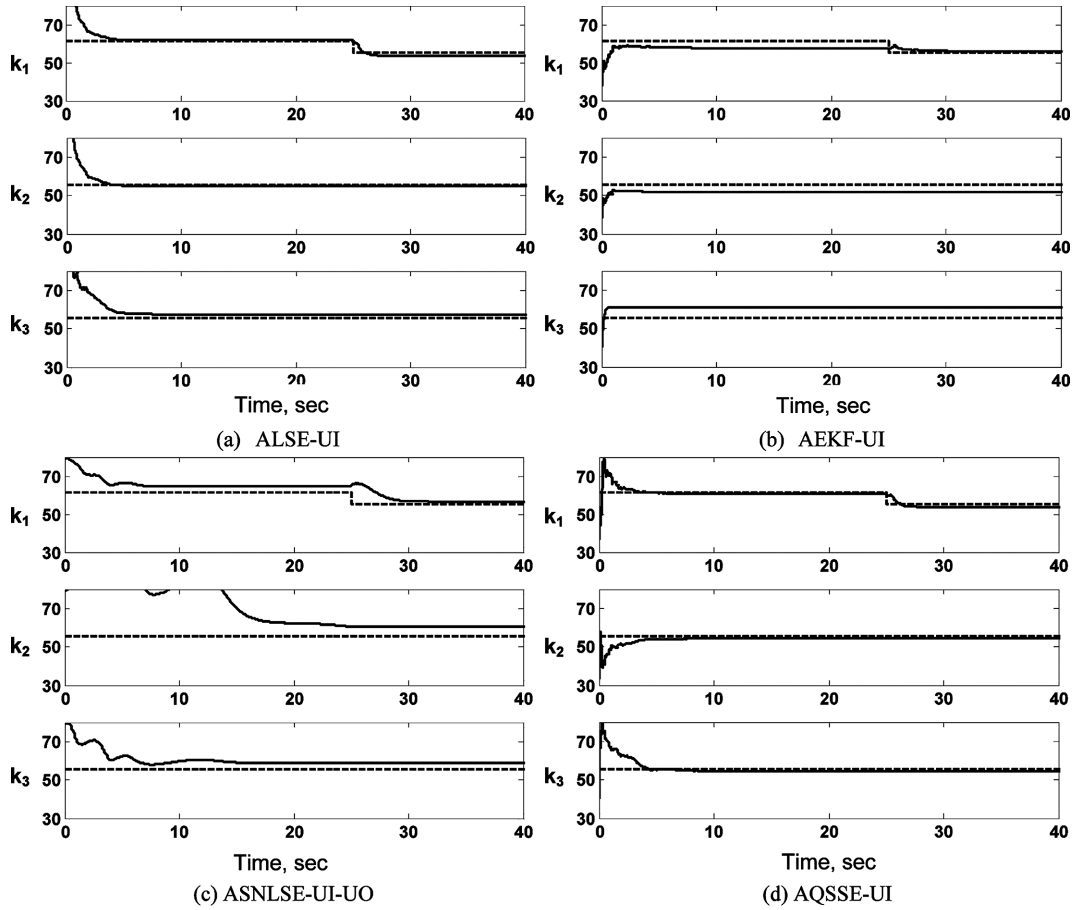

Fig. 6 Identified stiffness parameters (k_i in kN/m) for Damage Case 1 using different approaches with unknown input; (a) ALSE-UI, (b) AEKF-UI, (c) ASNLSE-UI-UO and (d) AQSSE-UI

Similar observations are obtained from Figs. 6-8 and Table 4 as that for the known input scenario: (i) the identified stiffness based on each approach agree with that of the referenced values, and (ii) with the unknown input, all the approaches investigated are still capable of tracking both the stiffness parameters and their variations due to damage. However, for the application of the ALSE-

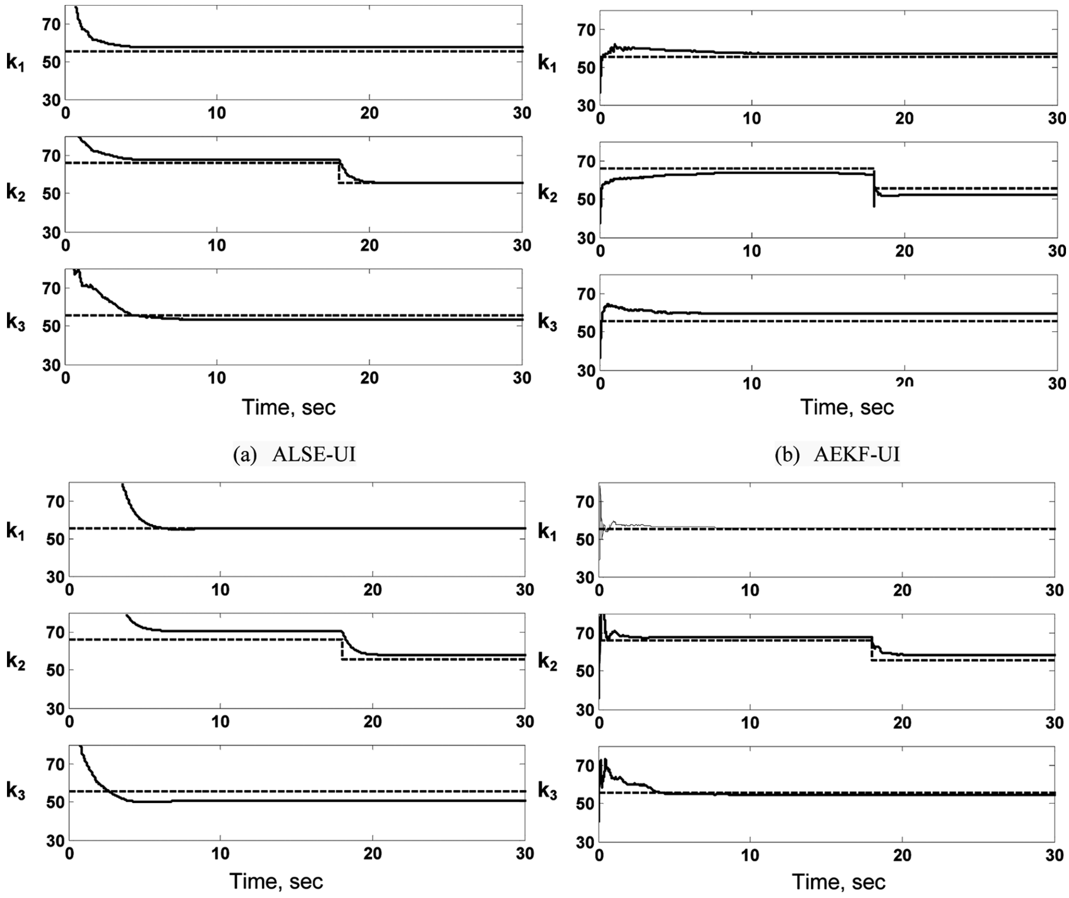

(a) ALSE-UI (b) AEKF-UI

(c) ASNLSE-UI-UO (d) AQSSE-UI

Fig. 7 Identified stiffness parameters (k_i in kN/m) for Damage Case 2 using different approaches with unknown input; (a) ALSE-UI, (b) AEKF-UI, (c) ASNLSE-UI-UO and (d) AQSSE-UI

UI technique, all the responses, including acceleration, velocity and displacement have to be available. With only the measurements of acceleration responses, the AEKF-UI, ASNLSE-UI-UO and AQSSE-UI approaches can be used for the damage identification. However, similar to the case with EKF approach, the AEKF-UI approach requires that the estimates of the initial values of the unknown parameters should not be far away from their theoretical values in order to obtain convergent solutions, and also because of the large size of extended state vector **Z**, it involves considerable computational efforts. In this connection, the ASNLSE-UI-UO and AQSSE-UI approaches will overcome the drawbacks of the AEKF-UI approach by estimating the parametric vector and the state vector separately, such that much smaller size of vectors and matrices are involved in the computation, which make these two approaches more efficient than the AEKF-UI approach.

Consequently, in the case of unknown inputs, the ASNLSE-UI-UO and AQSSE-UI techniques are again shown to be more suitable for the damage identification of structures among the four approaches investigated in this study, in terms of accuracy, convergence and efficiency. Further, for the ASNLSE-UI-UO technique, the convergence of the solutions is expected to be faster as the

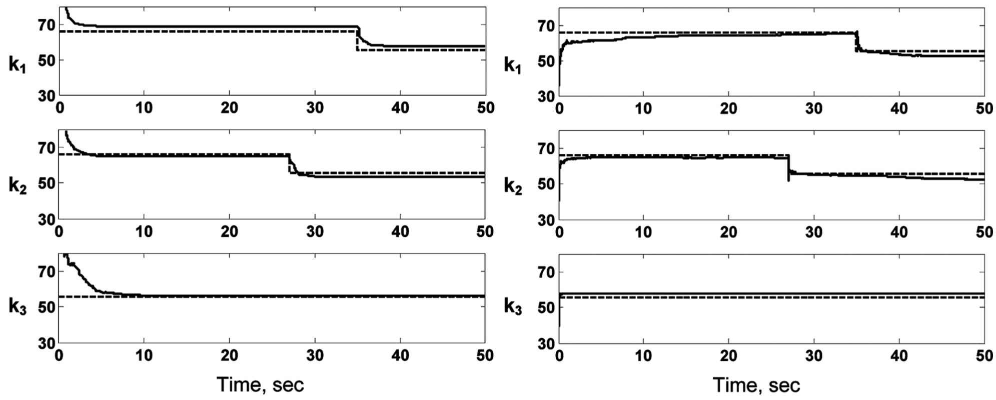

(a) ALSE-UI (b) AEKF-UI

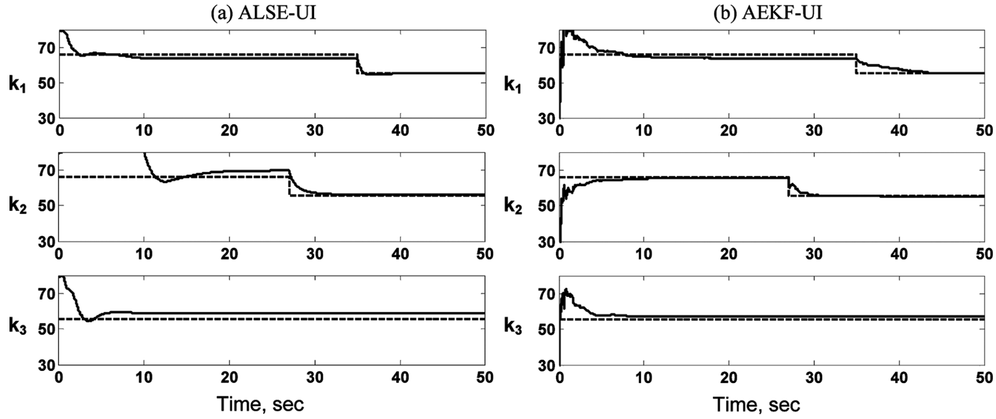

(c) ASNLSE-UI-UO (d) AQSSE-UI

Fig. 8 Identified stiffness parameters (k_i in kN/m) for Damage Case 3 using different approaches with unknown input; (a) ALSE-UI, (b) AEKF-UI, (c) ASNLSE-UI-UO and (d) AQSSE-UI

Table 4.1 Identified stiffness parameters before damage for all Damage Cases (unknown input)

		ALSE-UI		AEKF-UI		ASNLSE-UI-UO		AQSSE-UI	
Case 1	Ref. values	Predicted	Difference (%)	Predicted	Difference (%)	Predicted	Difference (%)	Predicted	Difference (%)
k1	61.5	62.02	0.85	64.92	5.56	64.84	5.42	60.94	0.90
k2	55.5	55.16	0.62	51.78	6.71	60.52	9.04	54.33	2.11
k3	55.5	57.36	3.35	51.11	7.91	58.72	5.81	54.55	1.72
Case 2	Ref. values	Predicted	Difference (%)	Predicted	Difference (%)	Predicted	Difference (%)	Predicted	Difference (%)
k1	55.5	57.52	3.64	56.98	2.67	55.28	0.39	56.06	1.00
k2	66	67.73	2.62	62.24	5.69	70.41	6.68	67.62	2.46
k3	55.5	53.33	3.91	59.96	8.03	50.38	9.23	54.68	1.47
Case 3	Ref. values	Predicted	Difference (%)	Predicted	Difference (%)	Predicted	Difference (%)	Predicted	Difference (%)
k1	66	68.85	4.32	64.54	2.22	63.57	3.67	63.76	3.40
k2	66	64.97	1.57	64.19	2.74	69.60	5.45	65.34	1.00
k3	55.5	56.23	1.31	57.78	4.11	58.80	5.94	57.20	3.06

Table 4.2 Identified stiffness parameters after damage for all Damage Cases (unknown input)

		ALSE-UI		AEKF-UI		ASNLSE-UI-UO		AQSSE-UI	
Case 1	Ref. values	Predicted	Difference (%)	Predicted	Difference (%)	Predicted	Difference (%)	Predicted	Difference (%)
k1	55.5	53.45	3.70	52.14	6.05	56.64	2.05	53.52	3.56
k2	55.5	55.16	0.62	51.77	6.71	60.52	9.04	54.33	2.11
k3	55.5	57.36	3.35	51.11	7.90	58.72	5.81	54.55	1.72
Case 2	Ref. values	Predicted	Difference (%)	Predicted	Difference (%)	Predicted	Difference (%)	Predicted	Difference (%)
k1	55.5	57.52	3.64	56.97	2.65	55.28	0.39	56.06	1.00
k2	55.5	55.50	0.01	58.74	5.84	57.88	4.29	58.28	5.02
k3	55.5	53.33	3.91	59.97	8.05	50.38	9.23	54.68	1.47
Case 3	Ref. values	Predicted	Difference (%)	Predicted	Difference (%)	Predicted	Difference (%)	Predicted	Difference (%)
k1	55.5	57.72	4.00	52.34	5.70	55.17	0.60	55.27	0.42
k2	55.5	53.36	3.86	52.51	5.39	56.17	1.20	55.14	0.64
k3	55.5	56.23	1.31	57.78	4.11	58.80	5.94	57.20	3.07

Table 5 Comparison of damage identification approaches

	ALSE/ALSE-UI	AEKF/AEKF-UI	ASNLSE/ASNLSE-UI-UO	AQSSE/AQSSE-UI
Characteristics	Time domain techniques for on-line or almost on-line damage identification			
Requirements	Measurement of acceleration and state vector **X**	Measurement of acceleration	Measurement of acceleration	Measurement of acceleration
Advantages	(i) Computational effort is less involved, and (ii) Solution is stable and convergent	Do not require measurement of **X**	(i) Do not require measurement of **X**, (ii) θ and **X** are obtained sequentially, the computational effort is reduced, and (iii) Solution is stable and convergent	(i) Do not require measurement of **X**, (ii) θ and **X** are obtained sequentially, the computational effort is reduced, and (iii) Solution is stable and convergent
Disadvantages	State vector **X** should be given or measured	(i) Dimension of **Z** is large so that computational effort is quite involved, and (ii) The convergence of the solution depends on the initial value of **Z**	Estimation of state vectors using Newmark-β method depends on the sampling frequency	

sampling frequency increases. The advantages and disadvantages of each approach are summarized in Table 5.

5. Conclusions

In this paper, comparisons of the ALSE-UI, AEKF-UI, ASNLSE-UI-UO and AQSSE-UI approaches for their capability in tracking the variations of structural parameters have been carried out, based on experimental test data. The experimental results were obtained using a scaled 3-story building model with a white noise excitation applied to the top floor (Zhou *et al.* 2008). Different damage scenarios and three damage cases had been tested, and the test data have been used to show the capability of each approach for structural damage tracking. The identification results for the stiffness of all stories, based on each approach for both known input and unknown input scenarios have been compared with the referenced values predicted by the finite-element model. This preliminary study demonstrates that the ASNLSE-UI-UO and AQSSE-UI approaches have advantages over the ALSE-UI and AEKF-UI approaches in terms of the accuracy, efficiency and practicality. Further studies will be conducted based on more experimental data.

Acknowledgements

This research is partially supported by the U.S. National Science Foundation Grant No. NSF-CMMI-0853395, and the National Natural Science Foundation of China Grant Nos. 50808138 and 50478037.

References

Alvin, K.F., Robertson, A.N., Reich, G.W. and Park, K.C. (2003), "Structural system identification: from reality to models", *Comput. Struct.*, **81**(12), 1149-1176.

Bernal, D. and Beck, J. (Ed.) (2004), "Preface to the special issue on phase I of the IASC-ASCE structural health monitoring benchmark", *J. Eng. Mech.-ASCE*, **130**(1), 1-2.

Chang, F.K. (Ed.) (2005), "Structural Health Monitoring", *Proceedings of the 5th International Workshop on Structural Health Monitoring*, Stanford University, Stanford, CA, USA, September.

Doebling, S.W., Farrar, C.R. and Prime, M.B. (1998), "A summary review of vibration-based damage identification methods", *Shock Vib. Digest*, **30**(2), 91-105.

Goodwin, G.C. and Sin, K.S. (1984), *Adaptive Filtering, Prediction and Control*, Prentice-Hall, Englewood, Cliffs, NJ, USA.

Hoshiya, M. and Saito, E. (1984), "Structural identification by extended Kalman filter", *J. Eng. Mech.-ASCE*, **110**(12), 1757-1770.

Huang, H.W. (2006), *System Identification and Damage Detection of Structures*, PhD dissertation, Depatement of Civil and Environental Engineering, University of California, Irvine, CA, USA.

Huang, H.W., Yang, J.N. and Zhou, L. (2010), "Adaptive quadratic sum-squares error with unknown inputs for structural damage identification", *Struct. Control Health Monit.*, **17**(4), 404-426.

Lin, J.W., Betti, R., Smyth, A.W. and Longman, R.W. (2001), "On-line identification of non-linear hysteretic structural systems using a variable trace approach", *Earthq. Eng. Struct. D.*, **30**(9), 1279-1303.

Loh, C.H., Lin, C.Y. and Huang, C.C. (2000), "Time domain identification of frames under earthquake loadings", *J. Eng. Mech.-ASCE*, **126**(7), 693-703.

Sato, T., Honda, R. and Sakanoue, T. (2001), "Application of adaptive Kalman filter to identify a five story frame structure using NCREE experimental data", *Proceedings of 8th International Conference on Structural Safety and Reliability (ICOSSAR 2001)*, Newport Beach, CA, USA, June.

Smyth, A.W., Masri, S.F., Kosmatopoulos, E.B., Chassiakos, A.G. and Caughey, T.K. (2002), "Development of adaptive modeling techniques for non-linear hysteretic systems", *Int. J. Nonlinear Mech.*, **37**(8), 1435-1451.

Wang, D. and Haldar, A. (1994), "Element-level system identification with unkown input", *J. Eng. Mech.-ASCE*, **120**(1), 159-176.

Wang, D. and Haldar, A. (1997), "System identification with limited observations and without input", *J. Eng. Mech.-ASCE*, **123**(5), 504-511.

Yang, J.N., Kim, J.H. and Agrawal, A.K. (2000), "Resetting semiactive stiffness damper for seismic response control", *J. Struct. Eng.-ASCE*, **126**(12), 1427-1433.
Yang, J.N. and Lin, S.L. (2004), "On-line identification of nonlinear hysteretic structures using an adaptive tracking technique", *Int. J. Nonlinear Mech.*, **39**(9), 1481-1491.
Yang, J.N. and Lin, S.L. (2005), "Identification of parametric variations of structures based on least squares estimation and adaptive tracking technique", *J. Eng. Mech.-ASCE*, **131**(3), 290-298.
Yang, J.N., Lin, S.L., Huang, H.W. and Zhou, L. (2006a), "An adaptive extended Kalman filter for structural damage identification", *Struct. Control Health Monit.*, **13**(4), 849-867.
Yang, J.N., Huang, H.W. and Lin, S.L. (2006b), "Sequential non-linear least-square estimation for damage identification of structures", *Int. J. Nonlinear Mech.*, **41**(1), 124-140.
Yang, J.N., Pan, S.W. and Lin, S.L. (2007a), "Least-squares estimation with unknown excitations for damage identification of structures", *J. Eng. Mech.-ASCE*, **133**(1), 12-21.
Yang, J.N., Pan, S.W. and Huang, H.W. (2007b), "An adaptive extended Kalman filter for structural damage identifications II: unknown inputs", *Struct. Control Health Monit.*, **14**(3), 497-521.
Yang, J.N., Bobrow, J., Jabbari, F., Leavitt, J., Cheng, C.P. and Lin, P.Y. (2007c), "Full-scale experimental verification of resetable semi-active stiffness dampers", *Earthq. Eng. Struct. D.*, **36**(9), 1255-1273.
Yang, J.N. and Huang, H.W. (2007), "Sequential non-linear least square estimation for damage identification of structures with unknown inputs and unknown outputs", *Int. J. Nonlinear Mech.*, **42**(5), 789-801.
Yang, J.N., Huang, H.W. and Pan, S.W. (2009), "Adaptive quadratic sum-squares error for structural damage identification", *J. Eng. Mech.-ASCE*, **135**(2), 67-77.
Zhou, L., Wu, S.Y. and Yang, J.N. (2008), "Experimental study of an adaptive extended Kalman filter for structural damage identification", *J. Infrastruct. Syst.*, **14**(1), 42-51.

CC